Research Square

Preprints are preliminary reports that have not undergone peer review.
They should not be considered conclusive, used to inform clinical practice,
or referenced by the media as validated information.

Long-term organic fertilizer amendment improves citrus yield and quality in calcareous soil mainly by shaping the microbiome and mobilizing soil phosphorus

kai gong
hongxiu wang
chuan you
chenghui zheng
Wei Qian
Yao Pang
wanyun yang
hang yin
qunzhen Li
yao zeng
liangzhi peng
nanqi wang
Changpin Chun

chuncp@swu.edu.cn

Southwest University https://orcid.org/0009-0001-2140-830X

Research Article

Keywords: Citrus, Organic fertilizer, Microbiome, Plant growth prompting bacteria, Phosphorus, Fruit quality.

Posted Date: November 9th, 2026

DOI: https://doi.org/10.21203/rs.3.rs-11298151/v1

License: This work is licensed under a Creative Commons Attribution 4.0 International License.
Read Full License

Long-term organic fertilizer amendment improves citrus yield and quality in calcareous soil mainly by shaping the microbiome and mobilizing soil phosphorus

Author Information

Kai Gong[a, #], Hongxiu Wang[b], Chuan You[c], Chenhui Zheng[a], Wei Qian[a], Yao Pang[a], Wanyun Yang[a], Hang Yin[a], Qunzhen Li[a], Yao Zeng[a], Liangzhi Peng[a], Nanqi Wang[a, *], Changpin Chun[a, *]

Affiliations

[a]National Citrus Engineering Research Center, Chongqing Key Laboratory of Citrus, Citrus Research Institute, Southwest University, Chongqing, 400712, China. [b]Chongqing Agro-Tech Extension Station, Chongqing, 401121, China. [c]Jiangsu provincial key lab for solid organic waste utilization, Key lab of organic-based fertilizers of China, Jiangsu Collaborative Innovation Center for Solid Organic Wastes, Educational Ministry Engineering Center of Resource-saving fertilizers, Nanjing Agricultural University, Nanjing, 211800, China.

[#] Kai Gong and Hongxiu Wang contribute equally to this work.

***Corresponding author**

Correspondence to: Changpin Chun (chuncp@swu.edu.cn) Nanqi Wang (wnq13579@swu.edu.cn)

Abstract

Background and aims Citrus, the largest fruit globally, often encounters nutritional imbalances, notably phosphorus (P) deficiency, when cultivated in calcareous soil. Although organic fertilizers outperform inorganic alternatives in citrus production, their specific impacts and the microbiome's role in calcareous soil remain unclear. This study aimed to investigate the effects of rapeseed cakes (RC) and cow manure (CM) on citrus plant-soil performance and their correlations with microbiome composition and functional profiles.

Methods We conducted a 5-year long-term positioning field experiment on citrus under calcareous soil conditions. Field experiments combined with amplicon and metagenome sequencing were employed to analyze differences in plant-soil performance and rhizosphere microbiome traits under RC and CM treatments. Isolation-culture verification was further performed to validate the function of key differential microorganisms.

Results RC and CM supplementation enhanced fruit yield and quality while facilitating P utilization in calcareous soil, with CM showing a better improvement

effect. Both organic fertilizers induced significant alterations in rhizosphere microbiome composition and function. The genus *Cupriavidus* was significantly enriched in rhizosphere under organic fertilizer treatments. Isolation-culture verification confirmed it enhanced soil P availability by secreting organic acids, alkaline phosphatases and other enzymes, serving as plant-growth-promoting rhizobacteria for citrus.

Conclusion Our findings clarify the effects of rapeseed cakes and cow manure on citrus growth and soil P activation in calcareous soil, and reveal the key role of the rhizosphere microbiome represented by *Cupriavidus* in this process. This study advances our understanding of microbiome-mediated improvement of citrus growth and P utilization via organic fertilizer application.

Keywords

Citrus; Organic fertilizer; Microbiome; Plant growth prompting bacteria; Phosphorus; Fruit quality.

Statements and Declarations

The authors declare that they have no known competing financial interests or personal relationships that could have appeared to influence the work reported in this paper.

1. Introduction

Citrus, the world's largest fruit, is of significant importance for global trade and human health. Plants cultivated in calcareous soil often encounter nutrient deficiencies, notably phosphorus (P), which is immobilized by calcareous soil (Arvin, 2019; Mahender et al., 2019). It is a core element involved in energy metabolism, carbohydrate transport, and chlorophyll synthesis in plants and plays a crucial role in the formation of citrus fruit quality (Czech et al., 2020; Wu et al., 2021). To address nutrient deficiency, there is widespread reliance on excessive chemical fertilizer application, which causes environmental pollution, soil degradation, and reduced microbial activity (Rabalais et al., 2010). Long-term excessive application of chemical fertilizers can disrupt the balance of soil microbial communities. Notably, effective phosphorus release depends on microbial synergy, as phosphorus from chemical fertilizers is easily immobilized in soil in the absence of microbial activity, limiting citrus uptake and reducing fertilizer efficiency over time. (Xu et al., 2020). In contrast, organic fertilizers have been shown to enhance soil quality and increase citrus production and quality (Haokip et al., 2021). Previous studies have predominantly focused on elucidating organic fertilizer mechanisms, emphasizing plant physiological and molecular responses, as well as soil nutrient cycling (Duarte et al., 2012; Yang and Zhang, 2023). Compared to chemical fertilizers, organic fertilizers harbor numerous microorganisms and serve as carbon

sources for microbial activity (Lin et al., 2019). Moreover, nutrients in organic fertilizers are gradually released through microbial processes over an extended period (Lin et al., 2019). Hence, microbiomes significantly contribute to the effectiveness of organic fertilizers. However, in the context of organic fertilizer application in citrus cultivation, the specific role of the microbiome in enhancing fruit quality—particularly through improved plant nutrition—has been largely overlooked. Notably, research on calcareous soils in this regard remains scarce.

Soil microorganisms play a pivotal role in regulatingP cycling and its availability (Hu et al., 2023). There are two primary mechanisms to increase available P: (1) secreting organic acids, such as citric acid and formic acid, to solubilize inorganic P (Yao et al., 2018), and (2) secreting enzymes, notably phosphatase, to mineralize organically fixed P (Devi et al., 2022). Microbes also contribute to fruit quality (Song et al., 2015). Sangiorgio et al. (2022) demonstrated that both bulk- and rhizosphere-associated fungal microbiomes contributed to the total soluble sugar content and titratable acidity of fruits. Furthermore, the taste and aroma chemistry of tomatoes are associated with the relative abundance of bacteria in the root microbiome (Escobar Rodríguez et al., 2021).Therefore, profiling the structure and function of the microbiome offers new insights for enhancing citrus plant nutrition and quality.

In this study, we examined the impact of plant- and animal-derived organic fertilizers on the soil physicochemical properties, leaf nutrition, and fruit quality of citrus

cultivated in calcareous soil. Subsequently, we analyzed the microbial community structure via amplicon sequencing. We integrated these data with physicochemical parameters (including soil nutrients and fruit quality) to quantify the relative contributions of microbial communities and nutrient factors to fruit quality. Furthermore, we employed shotgun metagenomic sequencing to characterize microbial functional potential, thereby elucidating the mechanisms underlying microbe-mediated nutrient transformation, particularly phosphorus and iron mobilization. This study not only reveals the synergistic interaction between microbiomes and nutrients in enhancing citrus productivity and quality but also provides scientific evidence for the integrated nutrient management of citrus.

2. Materials and Methods

2.1 Experimental Basics

The study utilized 5-year-old normal "Orah mandarin" fruiting trees, serving as the base rootstock for Ruta "Citrange" and an intermediate rootstock for Trovita orange, as the experimental material for high grafting. It was conducted at a citrus orchard base in Chongqing, China (30°16′ N, 107°37′ E), which is characterized by a subtropical monsoon climate with an average rainfall of approximately 1200 mm and an average annual temperature of 17°C. The orchard soil was classified as calcareous purple soil with the following physicochemical properties: pH 8.1, organic matter 16.41 g kg^{-1}, available nitrogen 52.02 mg kg^{-1}, available phosphorus 28.08 mg kg^{-1}, available potassium 232.08 mg kg^{-1}, available calcium 7536.99 mg kg^{-1}, available magnesium 1207.64 mg kg^{-1}, available iron 12.76 mg kg^{-1}, available manganese 172.82 mg kg^{-1}, available zinc 7.39 mg kg^{-1}, available copper 1.58 mg kg^{-1}, and available boron 0.07 mg kg^{-1}. Based on the long-term stationary experiment initiated in 2018, this study conducted field research in 2021 and 2022, the experiment followed a randomized block design with two treatments and a chemical fertilizer control treatment: (1) CK: conventional chemical fertilizer (N: P_2O_5: K_2O=15:15:15, 2 kg per plant); (2) RC: conventional chemical fertilizer + hole-applied rapeseed cake fertilizer 5 kg per plant; and (3) CM: conventional chemical fertilizer + hole-applied cow manure fertilizer 20 kg per plant. Each

125 treatment was replicated three times in 2021 and four times in 2022. Organic
126 fertilizers were applied in mid-February, and a sprouting fertilizer (15–20 d before
127 spring sprouting) was applied once, amounting to 30%–40% of the total fertilizer for
128 the year; in early to mid-July, a strong fruit fertilizer (applied 7–10 d before autumnal
129 tips), totaling 40% of the annual fertilizer. In late September, over-wintering
130 fertilizers were applied, comprising 20% to 30% of the annual fertilizer.
131 Decomposed organic fertilizers were adopted in the experiment. Further details are
132 presented in Supplementary Table 1, where both organic fertilizers maintained the
133 same amount of added phosphorus.

134 **2.2 Fruit yield and quality**

135 The yield per tree (kg) was assessed during the fruit-ripening period in February
136 2022 and 2023. Samples were collected from the upper-middle of the citrus canopy
137 periphery in four directions: east, south, west, and north. Twenty fruits from five
138 trees were combined to form one sample. The weight of each fruit (g) was measured
139 using an electronic scale. Peel brightness (L), red-green difference (a*), and yellow-
140 blue difference (b*) were determined using a CR-10 handheld colorimeter (Konica,
141 Tokyo, Japan). Soluble solid content (%) was measured through applying an AITO
142 PAL-1 refractometer (ATAGO, Tokyo, Japan). The fruit titratable acid content (%)
143 was assessed via titration with a sodium hydroxide indicator, and the fruit solid-acid
144 ratio (soluble solids/titratable acid) was calculated. The vitamin C content of the fruit

145 (mg·100 mL^{-1}) was determined by 2.6-dichlorophenol-indophenol titration (Liao et
146 al., 2023).

147 **2.3 Leaf relative chlorophyll and nutrient content**

148 Mature leaves from the spring tips were collected in September 2021 and 2022. The
149 relative chlorophyll content (SPAD value) was measured using a SPAD-502
150 chlorophyll meter (Konica, Tokyo, Japan) (Li et al., 2020). The leaf nitrogen content
151 was determined using concentrated sulfuric acid digestion and KDY-9820 Kjeldahl
152 nitrogen determination (Tongrunyuan Electromechanical Technology, Beijing,
153 China), and phosphorus content was assessed via nitric acid-perchloric acid (5:1)
154 digestion and a TU-1901 UV spectrophotometer (Pudian General Instrument,
155 Beijing, China) at 700 nm. Potassium, calcium, magnesium, iron, manganese, and
156 zinc concentrations were determined through nitric acid-perchloric acid (5:1)
157 digestion and analyzed using 240FS AA flame atomic absorption spectrometry
158 (Agilent, CA, USA) (De Luna Souto et al., 2023).

159 **2.4 Soil physicochemical properties**

160 During the soil element stabilization period in September 2021 and 2022, a 40 cm
161 deep pit was excavated near the drip line of the citrus tree canopy. Approximately
162 400 g of soil from depths of 5–35 cm was uniformly collected and debris was
163 removed. Five random points were sampled from each collection, and the soil
164 samples were combined to form a 1 kg composite using a 4-partitioning method. The

samples were then transported to the laboratory, where they were naturally dried, crushed, and stored for soil nutrient analysis. The pH of the leachate was measured using a PB-10 acidimeter (Sartorius, Gottingen, Germany) (Xin et al., 2022). The organic matter content was determined using the oxidizing capacity method of potassium dichromate-sulfuric acid after decoction in a DK-S20 constant-temperature oil bath (Shenxian Constant-Temperature Equipment Plant, Shanghai, China). Alkaline dissolved nitrogen was assessed via the diffusion method. Available phosphorus in alkaline soil was determined using sodium bicarbonate leaching with a UV-visible spectrophotometer. Available potassium, available calcium, and available magnesium were determined using ammonium acetate leaching flame photometry (Mei et al., 2022). Available iron, available manganese, and available zinc copper in alkaline soil were analyzed via atomic absorption spectrometry after leaching with a DTPA solution in an SHA-B water-bath constant-temperature oscillator (Bo Xun Medical and Bio-technical Instrument, Shanghai, China) (Achiba et al., 2010).

2.5 Soil enzyme activity

Rhizosphere soil (rhizosphere) refers to the soil surrounding the plant root system, influenced by the roots and their secretions, and the remaining soil is termed bulk (bulk) (Prashar et al., 2014). Soil sampling for the assessment of soil enzyme activity and microbial community diversity was conducted in September 2022. The top 5 cm

of soil in the vicinity of the dripline was excavated along with the root system of citrus plants at four points. Larger soil particles adhering to the root system were removed by gentle shaking, and rhizosphere soil adhering to the fibrous roots was brushed off with a fine brush and then placed into sterile self-sealing bags to replicate the rhizosphere soil. An equivalent amount of bulk soil was collected from areas without root growth and each treatment was sampled four times. The soil samples were immediately transported to the laboratory with ice. Upon arrival, they were divided into two parts: one part was applied to assess soil enzyme activities, and the other was stored at -80°C to determine the microbial community diversity and metagenome. Soil acid phosphatase (ACP) and alkaline phosphatase (ALP) activities were determined via visible spectrophotometry following the procedures outlined in the Soil Alkaline Phosphatase (S-AKP/ALP) Activity Test Kit and Soil Acid Phosphatase (S-ACP/ALP) Activity Detection Kit (Solarbio, Beijing, China).

2.6 Determination of phosphate-solubilizing capacity of strains

Strains in the logarithmic growth phase were inoculated at an inoculation ratio of 1 % into inorganic-phosphorus medium and organic-phosphorus medium, respectively, and incubated with shaking at 180 rpm and 30 ℃ for 2 d. The bacterial suspension was adjusted to an OD_{600} of 1, and then centrifuged at 10000 rpm for 30 min. The supernatant was diluted 10-fold, and 2 mL of diluted supernatant was mixed thoroughly with 2 mL of molybdenum-antimony-anti chromogenic reagent. After

30 min of color-development reaction, the absorbance was determined at 880 nm. A phosphorus standard curve was generated using KH_2PO_4 standard solution. The phosphate-solubilizing capacities of the strain for inorganic phosphorus and organic phosphorus were calculated separately based on the standard curve and sample absorbance at 880 nm.

2.7 Pot-based functional verification assay of the functional strain

One-year-old *Citrus reticulata* cv. Orah mandarin seedlings with uniform growth status were selected, and the old shoots were pruned to a consistent plant height. Pot assays were performed using in-situ soil collected from the field. Strain C1 was shake-flask cultured to the mid-late logarithmic growth phase with fermentation broth OD_{600} of 0.8-1.0. The original fermentation broth was diluted 10-fold with sterile pure water for root-drenching inoculation of citrus seedlings. The control group received sterile blank medium subjected to the identical 10-fold dilution. Inoculation treatments were conducted at 7, 21 and 35 days after transplanting. After the new shoots were fully mature, samples of above-ground new shoots and underground lateral roots were collected.

2.8 Amplicon sequencing

Soil DNA was extracted using a FastDNA® Spin Kit for Soil (MP Biomedicals, Solon, OH, USA), following the manufacturer's instructions. The microbial community structure analysis was performed using 16S rRNA high-throughput

sequencing technology, conducted by the Shanghai Meiji Biomedicals Technology Co. The extracted soil DNA served as a template to amplify the bacterial 16S rRNA-specific V3-V4 variable region using the primer pair 515FmodF (GTGYCAGCMGCCGCGGGTAA) and 806RmodR (GGACTACNVGGGTWTCTAAT). Sequencing was performed on the MiSeq PE250 platform.

2.9 Metagenome sequencing

The soil DNA extraction and second-generation metagenome sequencing were performed by the Beijing Youji Technology Co. The soil DNA was extracted using the NucleoSpin Soil Kit (Macherey-Nagel, Germany), following the manufacturer's instructions. The DNA content was quantified using the Qubit dsDNA BR Assay kit (Invitrogen, USA) with a Qubit Fluorometer, and its quality was assessed using 1% agarose gel electrophoresis. The sample DNA (1 μg) was randomly sheared using Covaris and then size-selected for 200–400 bp fragments using magnetic beads. The sorted DNA fragments underwent end repair, 3′-end adenylation, adapter ligation, and PCR amplification, with subsequent purification of the PCR products using magnetic beads. The purified PCR products were denatured and cyclized using splint oligo sequences. The cyclized single-stranded DNA constituted the final DNA library, which was subjected to bipartite sequencing on the DNAseq PE150 platform with Q30 ≥ 80%.

2.10 Data statistics and analysis

Data organization was performed using Microsoft Excel 2021. Data analysis and graphs were conducted using RStudio 4.2.2. Visualization was performed using Adobe Illustrator 2021.

Physiological indicators such as yield, fruit quality, and leaf and soil nutrients, were analyzed using the Shapiro-Wilk normality test and Levene's test (Anderson, 2006) to evaluate the normality and homogeneity of variances before conducting ANOVA test. ANOVA test was performed on data that met the normal distribution and homogeneity of variance criteria, with post-hoc testing performed using Duncan's method. The Spearman correlation analysis was conducted due to the skewed distribution of the data. This is implemented using the psych package in R.

Amplicon upstream analysis was conducted using QIIME2 v 2022.8 (Bolyen et al., 2019). PCR primers and low-quality sequences were trimmed using the DADA2 workflow in the QIIME2. The remaining reads were denoised, merged, and characterized to generate amplicon sequence variant (ASV) tables. Representative sequences from the preprocessed data were classified using the pre-trained classifier SILVA (Silva release 138; 99% of OTUs 515F/806R sequences) (Bokulich et al., 2018), retaining only ASVs annotated at least at the phylum level and removing those annotated as chloroplasts or mitochondria. ASVs with a total abundance less than ten or present in fewer than six samples (25% of the samples) were filtered out.

The library size was standardized for each sample by scaling through ranked subsampling to a total of 53,129 reads per sample (Beule and Karlovsky, 2020). Representative sequences were further filtered based on the ASV table, followed by the generation of approximate maximum likelihood phylogenetic trees using FastTree 2.1.8 in QIIME2 with default parameters.

For high-throughput sequencing data, variance partitioning analysis (VPA) was first performed using the vegan package to quantify the relative contributions of two factor groups to citrus fruit quality: (1) nutrient input factors (including soil physicochemical properties) and (2) microbial factors (represented by genus-level microbial community composition from amplicon sequencing). The VPA was based on redundancy analysis (RDA) to decompose the total variance of fruit quality indicators into the independent contributions of the two factor groups and their interaction. The Kruskal-Wallis rank sum test was also employed for multiple comparisons to assess the differences between the groups, with post hoc tests including Dunnett's T3 test for multiple groups and Wilcoxon rank sum test for two groups. α-Diversity among treatments was characterized by richness (Chao1) and diversity (Shannon) indices, displayed as bar charts. The principal coordinate analysis (PCoA) based on the Bray–Curtis distance algorithm was performed to evaluate the between-group differences. Stacked histograms at the gate level were plotted using the tax_stackplot function in the amplicon package (Liu et al., 2023),

and UpSet plots were generated using the UpSetR package (Conway et al., 2017). The website https://huttenhower.sph.harvard.edu/galaxy/ can offer linear discriminant analysis (linear discriminant analysis Effect Size, LEfSe) to identify species producing significantly different effects across treatments (Segata et al., 2011). The Mantel test from the linkET package was employed to explore the correlations between soil physicochemical properties, leaf nutrients, and fruit yield quality with variations in bulk and rhizosphere soil bacteria. Finally, the Spearman coefficients were computed using the Pheatmap package to assess the relationships between soil physicochemical properties, leaf nutrients, fruit yield quality, and genus-level bacteria, and the results were visualized in a heatmap.

Raw metagenome sequencing data were subjected to quality control using the kneaddata process (version 0.7.4) to ensure contamination-free high-quality data for downstream analysis (Liu et al., 2021). This involved the removal of low-quality reads using Trimmonmatic (version 0.39) (Bolger et al., 2014), as well as the elimination of host, splice, and PCR contamination using Bowtie 2 (version 2.5.0) (Langmead and Salzberg, 2012). Taxonomic classification of metagenomic reads into bacteria, archaea, fungi, and viruses was achieved using Kraken2 (version 2.1.1) based on the k-mer algorithm (Lu et al., 2022). Each sequence was divided into multiple k-mers, mapped to the lowest common ancestor (LCA) of all reference genomes, and grouped into classifications to form a classification tree, with the

weight of each node representing the frequency of k-mers assigned to that classification. Each RTL (root-to-leaf) path score on the classification tree represents the cumulative weight, with the highest-scoring path determining the classification path and assigning a classification leaf label to the sequence. In the case of multiple paths with equal scores, the sequence was tagged with a common ancestor. Taxonomic abundance estimation was accurately conducted using Bracken (version 2.5.0) (Lu et al., 2022), with read counts converted to relative abundances for subsequent analysis. Metagenomic functional profiling was performed using HuMAnN3 (version 3.6.1) (Beghini et al., 2021). Pairwise comparisons and visualization of the differential metabolic pathways were performed using STAMP 2.1.3.

3. Results

3.1 Organic fertilizer improves plant-soil performance of citrus

The 2021-2022 field experiment result demonstrated that organic fertilizers improved fruit yield and citrus quality. In 2021, compared to the control, the animal-derived cow manure (CM) significantly increased the yield per plant by 66.25% and single fruit weight by 14.15% (Fig. 1A, $p<0.05$). In 2022, plant-derived rapeseed cake (RC) significantly enhanced single-fruit weight by 20.49% (Fig. 1A, $p<0.05$). Additionally, both CM and RC significantly reduced the titratable acid content of ripe fruits by 2022 (Fig. 1A, $p<0.05$). Vitamin C content increased in fruits treated with CM in 2021 and RC in 2022 (Fig. 1A, $p<0.05$). Nevertheless, the soluble solids exhibited no significant post-treatment differences (Fig. S1A). Overall, organic fertilizer application promoted the improvement of citrus yield and fruit quality, with CM exhibiting a better comprehensive improvement effect.

Organic fertilizer effectively alleviated leaf yellowing symptoms, as evidenced by a significant increase in the relative chlorophyll content (SPAD values; Fig. S1B). Therefore, we analyzed plant nutrition levels across different treatments. In 2022, RC significantly increased leaf phosphorus (P) concentration by 15.38% (Fig. 1B). In addition, RC also increased leaf iron (Fe) by 38.89%, calcium (Ca) by 27.58%, manganese (Mn) by 79.77%, and zinc (Zn) by 59.27% in 2021, as well as magnesium (Mg) by 68.75% in 2022. CM significantly enhanced leaf Fe by 33.94%

in 2021 and Mg by 106.25% in 2022 (Fig S1B). No significant differences were observed for other elements between the organic fertilizer treatment and control groups. Hence, organic fertilizer improved the nutritional status of citrus plants, with RC exhibiting superior effects compared to CM.

Organic fertilizers notably improved soil quality. After two years of application in 2022, CM significantly reduced soil pH by 7.10% and increased organic matter by 147.05%, whereas RC significantly increased organic matter by 59.37% in bulk soil (Fig. S1C). Regarding element availability, RC notably boosted available P by 61.30% in the rhizosphere (Fig. 1B). CM enhanced available P by 114.79% and Fe by 120.22% in bulk soil in 2022 (Figs. 1B and S1C). In the first year (2021), organic fertilizer did not affect element availability (Fig. S1C). The collective results of the plant and soil nutrition levels indicated that organic fertilizer promoted P utilization. Subsequently, we assessed the enzyme activity of acid phosphatase (ACP) and alkaline phosphatase (ALP), which contributed to P cycling in the soil. The results indicated that CM significantly promoted ALP activity rather than ACP activity in both the bulk and rhizosphere soils (Fig. 1D). The correlation analysis revealed a significant negative relationship between available P and pH (Spearman's ρ=-0.76, p=0.004) and positive relationships with ACP (ρ=0.66, p=0.018) and ALP activity (ρ=0.71, p=0.010) in bulk soil (Fig. S2). However, in the rhizosphere soil, available P presented no significant negative relationship with ACP activity (Spearman's ρ=-

0.31, p=0.331), but exhibited a significant positive relationship with ALP activity (ρ=0.62, p=0.033) (Fig. S2). ACP originated from both plants and the microbiome, whereas ALP originated primarily from microbiomes. Hence, the microbiome can play a role in improving P nutrition through the application of organic fertilizer in citrus plants.

To clarify whether the improvement in fruit yield and quality was driven by additional nutrient input from organic fertilizers or the superimposed effect of altered microbial community structure, we performed variation-partitioning analysis (VPA) by integrating significantly-differentiated fruit-related indicators, soil nutrient factors, and the top 50 microbial genus-level abundances. The VPA results revealed that phosphorus and iron exhibited relatively high explanatory power for the variations in fruit yield, single-fruit weight, and titratable acid (TA) content. Notably, the joint explanatory power of phosphorus nutrients and the microbiome was higher than that of other elements, with values of 0.084, 0.122 and 0.261 for yield, single-fruit weight and TA, respectively (Fig. 1D). These findings suggested that the coupling effect of phosphorus nutrition and the microbiome played a dominant role in regulating citrus fruit yield and quality under organic fertilizer application.

3.2 Organic fertilizer induces alterations in microbial community diversity and composition

The combined explanatory power of soil available phosphorus and the microbiome

is the core factor driving the variation in fruit quality, and the microbiome itself also exerts an independent contribution. Then, how do organic fertilizers alter the diversity, composition, and core taxa of soil microbial communities? For α-diversity at the ASV level, organic fertilizer did not affect the Chao1 index (indicative of richness) or Shannon index (indicative of diversity) (Fig. S3A). Significant differences were observed between the rhizosphere and bulk soils in both the Chao1 and Shannon indices (Fig. S3A). The principal coordinate analysis (PCoA) based on Bray–Curtis distance revealed significant differences between the bulk and rhizosphere soils (PERMANOVA R^2=0.1450, p=0.001, Fig. 2A), as well as between treatments in both the bulk (PERMANOVA R^2=0.3202, p=0.001, Fig. 2A) and rhizosphere soils (PERMANOVA, R^2=0.3591, p=0.005, Fig. 2A), indicating the substantial effects of rhizosphere compartments and organic fertilizers on the soil microbial community structure.

Organic fertilizers contributed to a shift in the soil bacterial community composition, identifying 3078 ASVs spanning 34 phyla, 89 classes, 200 orders, 303 families, and 553 genera through database alignment. Actinobacteriota emerged as the dominant species with an average relative abundance of 20.59% (Fig. S3B). Other notable phyla were Proteobacteria (18.73%), Acidobacteriota (13.01%), Crenarchaeota (12.43%), Chloroflexi (9.15%), and Firmicutes (8.87%). The upset analysis of ASVs across different treatments revealed 1391 shared ASVs were present in all soils, with

specific ASVs observed under different organic fertilizer treatments and locations. Notably, 123 ASVs were present only in the RC and CM treatments, 7 to RC treatment alone, 20 to bulk soil, and 6 to rhizosphere soil (Fig. S3C).

The LEfSe analysis utilized a screening threshold of LDA>3.0, $p<0.05$. In the rhizosphere, RC enrichment compared to control revealed two orders, four families, and seven genera, which encompassed *unclassified_f_Pseudonocardiaceae*, *uncultured_f_Roseiflexaceae*, *Fictibacillus*, *Dongia*, *Cupriavidus*, *mle1_7*, and *Candidatus_ Xiphinematobacter*. Similarly, in the bulk soil, RC enrichment highlighted one phylum, two classes, three orders, three families, and three genera, including *uncultured_p_Armatimonadota*, *unclassified_f_Myxococcaceae* and *Cupriavidus* (Fig. 2B).

In the rhizosphere, significant differences in CM were observed across one class, one order, three families, and four genera. The enriched genera included *unclassified_f_Pseudonocardiaceae*, *unclassified_f_Myxococcaceae*, and *Cupriavidus*, and the excluded genus was *Candidatus_Xiphinematobacter* (Fig. 2C). In the CM bulk soil, significant differences were evident in two phyla, three classes, seven orders, eleven families, and ten genera. The enriched genera included *unclassified_f_Salisediminibacteriaceae*, *Novibacillus*, *Dongia*, *Devosia,* and *uncultured_c_Alphaproteobacteria*, while the excluded genera comprised *Nocardioides*, *Pseudogracilibacillus*, *unclassified_f_Bacillaceae*, *Acidibacter*, and

Steroidobacter.

To clarify whether the rhizosphere microenvironment exerts a filtering effect on bacterial communities, this study further selected bacterial genera that were significantly enriched and had clear taxonomic status in the RC and CM treatments as the core research subjects, and analyzed their abundance distribution differences between rhizosphere soil and bulk soil. The results showed that *Cupriavidus* and *Dongia* had the highest abundance in the RC treatment and both exhibited significant rhizosphere enrichment characteristics; *Cupriavidus* also showed the highest abundance and a distinct rhizosphere enrichment effect in the CM treatment. In addition, *Nocardioides* and *Steroidobacter* showed significant rhizosphere exclusion characteristics (Fig. 2D).

3.3 Relationships between microbiome community and plant-soil parameters

First, we conducted Mantel's test to examine the association between the overall community structure and plant-soil parameters. These findings indicated that the microbiome community of rhizosphere soil, as opposed to bulk soil, exhibited a notable correlation with fruit quality and yield. Specifically, it demonstrated significant correlations with titratable acid content and plant nutrition level, as indicated by the relative chlorophyll content (characterized by SPAD value), along with leaf concentrations of Mg and Fe (Fig. 3A and 3B).

The microbial community structure of the bulk soil was significantly correlated with

organic matter, alkaline dissolved nitrogen, available calcium, available magnesium, available manganese, available zinc, and available phosphorus content ($p<0.01$). Additionally, there was a significant correlation between the pH and available iron ($p<0.05$). Conversely, the microbial community structure of the rhizosphere soil was significantly associated solely with the concentration of available P, with no significant correlations found with ACP and ALP activity (Table S2).

Examining the correlation between specific bacterial genera and plant-soil parameters can facilitate the identification of potential key microbial taxa. For this purpose, we focused on dominant genera, defined as those with a relative abundance exceeding 0.5% (44 in total), for the Spearman rank correlation analysis. In the rhizosphere soil, 13 genera were significantly correlated with yield and fruit quality (Fig. 3D), 17 genera indicated significant correlations with leaf nutrient elements (Fig. 3E), and 10 genera were significantly correlated with ACP, ALP activity, and available P concentration (Fig. 3F). Furthermore, 30 genera were significantly correlated with the soil physicochemical properties in the bulk soil (Fig. 3G).

Among all dominant microbial communities, *Cupriavidus* was the core genus with the highest abundance and significant enrichment in both rhizosphere and bulk soils of treatment groups. Correlation analysis showed that its relative abundance was significantly positively correlated with soil ALP activity and available phosphorus content in rhizosphere soil. No significant correlation was observed between the

genus abundance and leaf total phosphorus content, while a positive trend was detected. Its abundance also had a significant positive correlation with leaf SPAD value. In terms of fruit traits, the relative abundance of *Cupriavidus* was significantly positively correlated with single fruit weight and yield, and significantly negatively correlated with fruit titratable acid content.

3.4 Organic fertilizer treatment alters acid- and phosphorus-related metabolic pathways

Under the organic fertilizer treatment, soil pH decreased (Fig. S1), which was confirmed by microbial functional profiling. Thirty-eight metabolic pathways potentially associated with acids were identified, and their abundance mostly increased after organic fertilizer treatments, particularly in the rhizosphere compared to the bulk soil (Fig. 4A).

In the CM treatment group (Fig. 4C), significantly enriched pathways included tricarboxylic acid (TCA) cycle I (prokaryotic) (TCA), TCA cycle VII (acetate producer) (PWY-7254), glyoxylate bypass and TCA hyper pathway (TCA-GLYOX-BYPASS), 2-methylcitrate cycle II (PWY-5747), glycolysis, pyruvate dehydrogenase, TCA, and glyoxylate bypass hyper pathway (GLYCOLYSIS-TCA-GLYOX-BYPASS). Notably, the TCA, TCA-GLYOX-BYPASS, and PWY-5747 pathways were predominantly associated with *Cupriavidus*, constituting 4.65%, 4.63%, and 32.96% of their abundance, respectively (Fig. 4D).

ALP activity originating from microorganisms significantly increased under the organic fertilizer treatment (Fig. 1), potentially contributing to the increase in soil available P (Fig. S2). Therefore, the impact of microorganisms on the metabolic pathways associated with phosphorus metabolism under organic fertilizer treatment was further analyzed. The relative abundance in most of the 41 metabolic pathways potentially related to phosphorus increased notably after organic fertilizer treatment, particularly in the rhizosphere soil compared with the bulk soil (Fig. 4B). Among these pathways, phosphatidylcholine acyl editing (PWY-6803) was enriched in the rhizosphere soil under both RC and CM treatments as well as in the bulk soil under RC treatment. Additionally, the phospholipase (LIPASYN-PWY) pathway was enriched in the rhizosphere soil under both the RC and CM treatments (Fig. 4E). Furthermore, 93.19% of PWY-6803 originated from *Cupriavidus*, whereas LIPASYN-PWY was contributed by *Cupriavidus*, *Variovorax*, *Achromobacter*, *Bacillus*, and *Streptomyces*, accounting for 24.17%, 0.81%, 0.31%, 0.26%, and 0.16%, respectively (Fig. 4F).

Previous studies indicated that *Cupriavidus* could significantly promote phosphorus mobilization in citrus rhizosphere soil by regulating soil acidification processes and phosphorus-metabolic pathways. To further verify its phosphorus-mobilizing capacity, rhizosphere soil samples collected in 2022 were used for the isolation of culturable bacteria. A total of 142 bacterial

isolates belonging to 17 genera were obtained, among which three *Cupriavidus* strains were screened and designated as C1, C2 and C3. The 16S rRNA gene sequences of the three isolates and 13 reference sequences of *Cupriavidus* retrieved from the NCBI database were trimmed to identical amplified regions for sequence alignment and phylogenetic tree construction, with *Bacillus subtilis* used as the out-group for tree rooting. Meanwhile, sequence similarity comparison was performed between the isolates and *Cupriavidus* ASVs derived from rhizosphere amplicon sequencing (Fig. 5A).

3.5 Identification and pot-based functional verification of *Cupriavidus* isolates

Previous studies have demonstrated that *Cupriavidus* can significantly promote phosphorus mobilization in citrus rhizosphere soil by modulating soil acidification processes and phosphorus-metabolic pathways. To further validate its phosphorus-mobilizing potential, rhizosphere soil samples collected in 2022 were used for the isolation and screening of culturable bacteria. A total of 142 bacterial isolates affiliated to 17 genera were obtained, among which three *Cupriavidus* strains were recovered and designated as C1, C2 and C3. The 16S rRNA gene sequences of the three isolates and 13 *Cupriavidus* reference sequences retrieved from the NCBI database were trimmed to identical amplified regions for sequence alignment and

phylogenetic tree construction, with *Bacillus subtilis* employed as the out-group for tree rooting. Meanwhile, sequence identity analysis was performed between the isolates and *Cupriavidus* ASVs derived from rhizosphere amplicon sequencing (Fig 5A).

Among these candidate strains, strain C1 possessed the highest phosphate-solubilizing capacity for both inorganic and organic phosphorus sources, and exhibited 100 % sequence identity with the *Cupriavidus* ASV detected by amplicon sequencing (Fig 5B). Accordingly, strain C1 was selected for pot-based functional verification assays. Compared with the CK control treatment, rhizosphere available phosphorus content increased by 14.58 % and leaf phosphorus concentration increased by 20.89 % following inoculation with strain C1. Meanwhile, the above-ground new-shoot biomass and underground lateral-root biomass were higher than those of the control group, with increments of 20.16 % and 8.54 %, respectively (Fig 5C).

4. Discussion

Organic fertilizer significantly enhanced the plant-soil P and Fe nutrition levels of citrus (Fig. 1), likely due to soil acidification and microbiome activity (Figs. 3-4). In this study, soil pH availability was significantly correlated with P and Fe availability, (Fig. 3). Specifically, P availability decreased as the soil pH increased from 7.5 to 8.5 (Lambers and Oliveira, 2019). The reduced P availability in calcareous soils was attributed to the reaction of P with Ca, where P-Ca solubility is the lowest at pH=8.0 (Lambers and Oliveira, 2019). Moreover, Fe solubility decreased by 1000-fold with each unit increase in soil pH within a pH range of 4–9 (Tsai and Schmidt, 2020). The application of CM significantly lowered the soil pH from 8.25 to 7.73, which was favorable for citrus cultivation, as citrus prefers slightly acidic soils (Zhang et al., 2018). Although RC (pH 5.30) was more acidic than CM (pH 5.8) (Table S1), RC application did not affect soil pH (Fig. S1). One reason could be that the application amount of RC was four times higher than that of CM, as the major nutrient concentration of RC were 3–3.87 times lower than that of CM. A higher amount of acidic organic material resulted in better soil acidification. Another reason could be the higher secretion of organic acids from the microbiome, as revealed by the metagenomic analysis (Fig. 4). Organic fertilizers, particularly CM, increased the abundance of small-molecule organic acid-related metabolic pathways, with higher expression observed in the rhizosphere soil (Fig. 4). P-solubilizing microorganisms

550 can produce organic acids that can be crucial for mineral P solubilization as
551 metabolic pathway intermediates, including gluconic, 2-ketogluconic, oxalic, acetic,
552 citric, succinic, and glyuronic acids (Khan et al., 2009). After CM treatment, the
553 abundance of five pathways significantly increased: TCA cycle I (prokaryotic), TCA
554 cycle VII (acetic acid producer), glyoxylate bypass and TCA hyper pathway, 2-
555 methylcitrate cycle II, glycolysis, pyruvate dehydrogenase, TCA, and glyoxylate
556 bypass hyper pathway (Fig. 4). All four pathways are involved in the TCA cycle, in
557 which organic acids, such as citric acid, succinic acid, and malic acid, are
558 synthesized (Yin et al., 2015). The 2-methylcitric acid cycle is a widely distributed
559 carbon metabolic pathway that efficiently converts propionate and propionyl-CoA
560 into succinic acid and pyruvate, respectively (Rocco and Escalante-Semerena, 2010).
561 Succinic acid dissolves insoluble phosphates (Scervino et al., 2010). As the
562 microbiome exhibits consistent activity, acidification by the microbiome occurs over
563 a prolonged duration, resulting in a gradual effect.
564 Microbiome enzyme activity plays a crucial role in soil P transformation. In this
565 study, ALP activity consistently exceeded ACP activity (Fig. 1). This may be
566 attributed to the pH dependence of phosphatase activity, with alkaline conditions
567 favoring ALP activity (Ragot et al., 2017). Because ALP is solely secreted by the
568 microbiome (Nannipieri et al., 2011), microbiome-derived ALP played a
569 predominant role, which is consistent with previous studies (Luo et al., 2017; Wang

et al., 2012). Metagenomic analysis also indicated an increase in the abundance of P metabolism-related pathways induced by organic fertilizers, particularly in the rhizosphere (Fig. 4). Specifically, both organic fertilizers enriched phosphatidylcholine acyl editing and phospholipase pathways in rhizosphere soil (Fig. 4). Phospholipases can release P from organic sources, thereby facilitating plant growth (Tapia-Torres et al., 2016). ACP is secreted by plants and microorganisms (Nannipieri et al., 2011). P-deficiency stress can notably elevate ACP activity in the plant rhizosphere, serving as a critical mechanism for plants to acquire P in low P environments (Spohn and Kuzyakov, 2013). In this study, the reduction in rhizosphere ACP activity following organic fertilizer application may be attributed to improved P nutrition in citrus, resulting in decreased ACP secretion by citrus plants. Overall, the combination of soil enzyme activity and metagenomic analysis suggested that microbiome activity contributed to the enhancement of P availability induced by organic fertilizers.

The microbiome composition of the rhizosphere soil, presented a significant correlation with citrus fruit quality and plant nutrition level (Fig. 3). The microbial community can explain the variation in fruit quality through its independent effect or through synergistic interaction with rhizosphere nutrients (Fig. 3E). Therefore, investigating the diversity of rhizobacterial composition can be essential to understanding the role of the microbiome in citrus plant performance. The

composition and function of rhizosphere microbiomes are influenced by the physiological state of the plants through root exudates (Zhou et al., 2020). Conversely, rhizosphere microbiomes can affect plant nutrition, yield, and quality (Kumar and Dubey, 2020). In this study, the composition and function of rhizosphere microbiomes were analyzed in September during the critical period for citrus fruit quality development, whereas fruit quality was assessed during the fruit-ripening period in the following months of February. Microbiome profiling was conducted nearly five months in advance, based on the developmental stages of fruit quality. *Dongia*, *Cupriavidus*, and *Streptomyces* emerged as the top candidate genera for enhancing citrus plant nutrition, as they were enriched by organic fertilizers and showed positive correlations with plant nutrition, yield, and fruit quality (Figs. 2 and 3). The metagenomic analysis provided evidence for potential plant growth promoting rhizobacteria, with enriched organic acid metabolic pathways primarily attributed to the genus *Cupriavidus* (Fig. 4). Additionally, after organic fertilizer treatment, there was a notable increase in phosphorus-related metabolic pathways, particularly in rhizosphere soil. Both the phosphatidylcholine acyl-editing and phospholipase pathways, which contributed to fatty acid and lipid biosynthesis, exhibited significant increases after RC and CM treatment, with phospholipases also capable of releasing phosphorus from organophosphates (Tapia-Torres et al., 2016). The analysis of these two pathways revealed predominant contributions from

610 *Cupriavidus*, *Variovorax*, *Achromobacter*, *Bacillus*, and *Streptomyces*. A significant
611 positive correlation between *Cupriavidus* and *Streptomyces* and the rhizosphere soil
612 available phosphorus content was evident (Fig. 3). Consequently, their metabolic
613 activities could induce soil insoluble phosphorus dissolution through organic acid
614 secretion, and the secretion of phospholipases and other enzymes may facilitate
615 organophosphate mineralization. Cabrera-Rodríguez et al. (2020) observed a marked
616 increase in the relative abundance of *Dongia* in pecan plantations with the
617 application of organic fertilizer. Prior research has indicated that *Cupriavidus* is the
618 predominant genus harboring *phoC* in soils (Zheng et al., 2019), where *phoC*-
619 carrying bacteria played a vital role in enhancing soil phosphorus availability
620 through acid phosphatase secretion. *Cupriavidus* nantongensis X1 can degrade
621 propylene phosphorus residues in insecticides, thereby mitigating environmental
622 contamination (Fang et al., 2023). Moreover, the *Cupriavidus* metallidurans CH34
623 strain is resilient to harsh heavy-metal conditions abundant in heavy metals (Janssen
624 et al., 2010). The *phoD* gene encodes alkaline phosphatase (Jiang et al., 2022), and
625 its functional microbial populations were more abundant in soils treated with organic
626 materials than in those receiving chemical fertilizer. *Streptomyces* is the principal
627 genus encoding *phoD* functional microorganisms (Luo et al., 2019). Therefore,
628 *Dongia*, *Cupriavidus*, and *Streptomyces* are plant growth promoting rhizobacteria
629 (PGPRs) and prospective functional strain candidates. In future studies,

representative strains from these genera should be selectively isolated from the rhizosphere soil and reintroduced into citrus rhizosphere settings under field conditions to validate their biological efficacy.

5. Conclusion

This study found that both RC and CM can regulate the composition and function of the microbial community, and act synergistically with soil nutrients (primarily available phosphorus), thereby increasing citrus yield and improving fruit quality (Fig. 6). However, CM outperformed RC in terms of increasing yield, improving fruit quality, enhancing soil nutrients, and increasing enzyme activity, and its regulatory effects on microbial community composition and function were also more significant. Therefore, in citrus cultivation in calcareous soil, CM is more suitable than RC. Notably, the microbiome composition in the rhizosphere soil, rather than in the bulk soil, correlated significantly with citrus performance. *Cupriavidus* could be potential plant growth-promoting rhizobacteria for citrus, enhancing soil nutrient availability, facilitating leaf nutrient absorption, and improving fruit quality. In summary, our study explained the role of the microbiome in enhancing citrus yield and quality through organic fertilizer application.

References

Achiba, W.B., Lakhdar, A., Gabteni, N., Laing, G.D., Verloo, M., Boeckx, P., Van Cleemput, O., Jedidi, N., Gallali, T., 2010. Accumulation and fractionation of trace metals in a Tunisian calcareous soil amended with farmyard manure and municipal solid waste compost. J. Hazard. Mater. 176, 99–108.

Anderson, M.J., 2006. Distance-based tests for homogeneity of multivariate dispersions. Biometrics 62, 245–253.

Arvin, P., 2019. Study of different levels of nitrogen, phosphorus and potassium on physiological and morphological parameters and essential oils in savory plant. J. Plant Res. 32(2).

Beghini, F., McIver, L.J., Blanco-Míguez, A., Dubois, L., Asnicar, F., Maharjan, S., Mailyan, A., Manghi, P., Scholz, M., Thomas, A.M., Valles-Colomer, M., Weingart, G., Zhang, Y., Zolfo, M., Huttenhower, C., Franzosa, E.A., Segata, N., 2021. Integrating taxonomic, functional, and strain-level profiling of diverse microbial communities with bioBakery 3. eLife 10, e65088.

Beule, L., Karlovsky, P., 2020. Improved normalization of species count data in ecology by scaling with ranked subsampling (SRS): application to microbial communities. PeerJ 8, e9593.

Bokulich, N.A., Kaehler, B.D., Rideout, J.R., Dillon, M., Bolyen, E., Knight, R., Huttley, G.A., Gregory Caporaso, J., 2018. Optimizing taxonomic classification of marker-gene amplicon sequences with QIIME 2's q2-feature-classifier plugin. Microbiome 6, 90.

Bolger, A.M., Lohse, M., Usadel, B., 2014. Trimmomatic: a flexible trimmer for Illumina sequence data. Bioinformatics 30, 2114–2120.

Bolyen, E., Rideout, J.R., Dillon, M.R., Bokulich, N.A., Abnet, C.C., Al-Ghalith, G.A., Alexander, H., Alm, E.J., Arumugam, M., Asnicar, F., Bai, Y., Bisanz, J.E., Bittinger, K., Brejnrod, A.,

Brislawn, C.J., Brown, C.T., Callahan, B.J., Caraballo-Rodríguez, A.M., Chase, J., Cope, E.K., Da Silva, R., Diener, C., Dorrestein, P.C., Douglas, G.M., Durall, D.M., Duvallet, C., Edwardson, C.F., Ernst, M., Estaki, M., Fouquier, J., Gauglitz, J.M., Gibbons, S.M., Gibson, D.L., Gonzalez, A., Gorlick, K., Guo, J., Hillmann, B., Holmes, S., Holste, H., Huttenhower, C., Huttley, G.A., Janssen, S., Jarmusch, A.K., Jiang, L., Kaehler, B.D., Kang, K.B., Keefe, C.R., Keim, P., Kelley, S.T., Knights, D., Koester, I., Kosciolek, T., Kreps, J., Langille, M.G.I., Lee, J., Ley, R., Liu, Y.-X., Loftfield, E., Lozupone, C., Maher, M., Marotz, C., Martin, B.D., McDonald, D., McIver, L.J., Melnik, A.V., Metcalf, J.L., Morgan, S.C., Morton, J.T., Naimey, A.T., Navas-Molina, J.A., Nothias, L.F., Orchanian, S.B., Pearson, T., Peoples, S.L., Petras, D., Preuss, M.L., Pruesse, E., Rasmussen, L.B., Rivers, A., Robeson, M.S., Rosenthal, P., Segata, N., Shaffer, M., Shiffer, A., Sinha, R., Song, S.J., Spear, J.R., Swafford, A.D., Thompson, L.R., Torres, P.J., Trinh, P., Tripathi, A., Turnbaugh, P.J., Ul-Hasan, S., van der Hooft, J.J.J., Vargas, F., Vázquez-Baeza, Y., Vogtmann, E., von Hippel, M., Walters, W., Wan, Y., Wang, M., Warren, J., Weber, K.C., Williamson, C.H.D., Willis, A.D., Xu, Z.Z., Zaneveld, J.R., Zhang, Y., Zhu, Q., Knight, R., Caporaso, J.G., 2019. Reproducible, interactive, scalable and extensible microbiome data science using QIIME 2 Nat. Biotechnol. 37, 852–857.

Cabrera-Rodríguez, A., Nava-Reyna, E., Trejo-Calzada, R., García-De la Peña, C., Arreola-Ávila, J.G., Collavino, M.M., Vaca-Paniagua, F., Díaz-Velásquez, C., Constante-García, V., 2020. Effect of organic and conventional systems used to grow pecan trees on diversity of soil microbiota. Diversity-Basel 12, 436.

Conway, J.R., Lex, A., Gehlenborg, N., 2017. UpSetR: an R package for the visualization of intersecting sets and their properties. Bioinformatics 33, 2938–2940.

693 Czech, A., Zarycka, E., Yanovych, D., Zasadna, Z., Grzegorczyk, I., Kłys, S., 2020. Mineral
694 content of the pulp and peel of various citrus fruit cultivars. Biol. Trace Elem. Res. 193, 555–
695 563.
696 De Luna Souto, A.G., Cavalcante, L.F., De Melo, E.N., Cavalcante, Í.H.L., Da Silva, R.Í.L., De
697 Lima, G.S., Gheyi, H.R., Pereira, W.E., De Paiva Neto, V.B., De Oliveira, C.J.A., De Oliveira
698 Mesquita, F., 2023. Salinity and mulching effects on nutrition and production of grafted sour
699 passion fruit. Plants-Basel.
700 Devi, R., Kaur, T., Kour, D., Yadav, A., Yadav, A.N., Suman, A., Ahluwalia, A.S., Saxena, A.K.,
701 2022. Minerals solubilizing and mobilizing microbiomes: A sustainable approach for
702 managing minerals' deficiency in agricultural soil. J. Appl. Microbiol. 133, 1245–1272.
703 Duarte, A.M., Caixeirinho, D., Miguel, M.G., Sustelo, V., Nunes, C., Fernandes, M.M., Marreiros,
704 A., 2012. Organic acids concentration in citrus juice from conventional versus organic
705 farming. Acta Hortic. 601–606.
706 Escobar Rodríguez, C., Novak, J., Buchholz, F., Uetz, P., Bragagna, L., Gumze, M., Antonielli,
707 L., Mitter, B., 2021. The bacterial microbiome of the tomato fruit is highly dependent on the
708 cultivation approach and correlates with flavor chemistry. Front. Plant Sci. 12, 775722.
709 Fang, L., Zhou, Y., Chen, T., Geng, Y., Li, Z., Zha, W., Shi, T., Hua, R., 2023. Efficient
710 biodegradation characteristics and detoxification pathway of organophosphorus insecticide
711 profenofos via *Cupriavidus nantongensis* X1T and enzyme OpdB. Sci. Total Environ. 862,
712 160782.
713 Haokip, S.W., Singh, B., Sheikh, K.A., Shankar, K., Debbarma, R., Lalrinngheta, J., Nengparmoi,
714 T., 2021. Growth and yield response to application of organic and inorganic nutrient sources
715 in lemon [*Citrus limon* (L.) Burm.] cv. Assam Lemon. Int J Plant Sci. 46–52.

716 Hu, X., Gu, H., Liu, J., Wei, D., Zhu, P., Cui, X., Zhou, B., Chen, X., Jin, J., Liu, X., Wang, G.,
717 2023. Metagenomic strategies uncover the soil bioavailable phosphorus improved by organic
718 fertilization in Mollisols. Agric. Ecosyst. Environ. 349, 108462.
719 Janssen, P.J., Houdt, R.V., Moors, H., Monsieurs, P., Morin, N., Michaux, A., Benotmane, M.A.,
720 Leys, N., Vallaeys, T., Lapidus, A., Monchy, S., Médigue, C., Taghavi, S., McCorkle, S.,
721 Dunn, J., Lelie, D. van der, Mergeay, M., 2010. The complete genome sequence of
722 *Cupriavidus metallidurans* strain CH34, a master survivalist in harsh and anthropogenic
723 environments. PLoS One 5, e10433.
724 Jiang, N., Wei, K., Pu, J., Zhang, Y., Xie, H., Bao, H., Chen, L., 2022. Effects of the reduction in
725 chemical fertilizers on soil phosphatases encoding genes (phoD and phoX) under crop residue
726 mulching. Appl. Soil Ecol. 175, 104428.
727 Khan, M.S., Zaidi, A., Wani, P.A., 2009. Role of phosphate solubilizing microorganisms in
728 sustainable agriculture - A Review. Agron. Sustain. Dev. 551–570.
729 Kumar, A., Dubey, A., 2020. Rhizosphere microbiome: Engineering bacterial competitiveness for
730 enhancing crop production. J. Adv. Res. 24, 337–352.
731 Lambers, H., Oliveira, R.S., 2019. Plant Physiological Ecology. Springer International Publishing,
732 Cham.
733 Langmead, B., Salzberg, S.L., 2012. Fast gapped-read alignment with Bowtie 2. Nat. Methods 9,
734 357–359.
735 Li, B., Wang, S., Zhang, Y., Qiu, D., 2020. Acid soil improvement enhances disease tolerance in
736 citrus infected by *Candidatus* Liberibacter asiaticus. IJMS 21, 3614.

Liao, L., Li, Y., Lan, X., Yang, Y., Wei, W., Ai, J., Feng, X., Chen, H., Tang, Y., Xi, L., Wang, Z., 2023. Integrative analysis of fruit quality and anthocyanin accumulation of Plum cv. 'Cuihongli' (*Prunus salicina* Lindl.) and its bud mutation. Plants-Basel 12, 1357.

Lin, W., Lin, M., Zhou, H., Wu, H., Li, Z., Lin, Wenxiong, 2019. The effects of chemical and organic fertilizer usage on rhizosphere soil in tea orchards. PLoS ONE 14, e0217018.

Lin, Y., Ye, G., Kuzyakov, Y., Liu, D., Fan, J., Ding, W., 2019. Long-term manure application increases soil organic matter and aggregation, and alters microbial community structure and keystone taxa. Soil Biol. Biochem. 134, 187–196.

Liu, Y., Chen, Lei, Ma, T., Li, X., Zheng, M., Zhou, X., Chen, Liang, Qian, X., Xi, J., Lu, H., Cao, H., Ma, X., Bian, B., Zhang, P., Wu, J., Gan, R., Jia, B., Sun, L., Ju, Z., Gao, Y., Wen, T., Chen, T., 2023. EasyAmplicon: An easy-to-use, open-source, reproducible, and community-based pipeline for amplicon data analysis in microbiome research. iMeta 2.

Liu, Y.-X., Qin, Y., Chen, T., Lu, M., Qian, X., Guo, X., Bai, Y., 2021. A practical guide to amplicon and metagenomic analysis of microbiome data. Protein Cell 12, 315–330.

Lu, J., Rincon, N., Wood, D.E., Breitwieser, F.P., Pockrandt, C., Langmead, B., Salzberg, S.L., Steinegger, M., 2022. Metagenome analysis using the Kraken software suite. Nat. Protoc. 17, 2815–2839.

Luo, G., Ling, N., Nannipieri, P., Chen, H., Raza, W., Wang, M., Guo, S., Shen, Q., 2017. Long-term fertilisation regimes affect the composition of the alkaline phosphomonoesterase encoding microbial community of a vertisol and its derivative soil fractions. Biol. Fertil. Soils 53, 375–388.

758 Luo, G., Sun, B., Li, L., Li, M., Liu, M., Zhu, Y., Guo, S., Ling, N., Shen, Q., 2019. Understanding
759 how long-term organic amendments increase soil phosphatase activities: Insight into phoD-
760 and phoC-harboring functional microbial populations. Soil Biol. Biochem. 139, 107632. 2
761 Mahender, A., Swamy, B.P.M., Anandan, A., Ali, J., 2019. Tolerance of iron-deficient and -toxic
762 soil conditions in rice. Plants-Basel 8, 31.
763 Mei, L., Zhang, N., Wei, Q., Cao, Y., Li, D., Cui, G., 2022. Alfalfa modified the effects of degraded
764 black soil cultivated land on the soil microbial community. Front. Plant Sci. 13, 938187.
765 Nannipieri, P., Giagnoni, L., Landi, L., Renella, G., 2011. Phosphorus in Action. Chapter 9: Role
766 of phophatase enzymes in soil. Springer-Verlag Berlin Heidelberg. 215–243.
767 Rabalais, N.N., Díaz, R.J., Levin, L.A., Turner, R.E., Gilbert, D., Zhang, J., 2010. Dynamics and
768 distribution of natural and human-caused hypoxia. Biogeosciences 7, 585–619.
769 Ragot, S.A., Kertesz, M.A., Mészáros, É., Frossard, E., Bünemann, E.K., 2017. Soil phoD and
770 phoX alkaline phosphatase gene diversity responds to multiple environmental factors. FEMS
771 Microbiol. Ecol. 93, fiw212.
772 Rocco, C.J., Escalante-Semerena, J.C., 2010. In salmonella enterica, 2-methylcitrate blocks
773 gluconeogenesis. J. Bacteriol. 192, 771–778.
774 Sangiorgio, D., Cellini, A., Donati, I., Ferrari, E., Tanunchai, B., Fareed Mohamed Wahdan, S.,
775 Sadubsarn, D., Farneti, B., Checcucci, A., Buscot, F., Spinelli, F., Purahong, W., 2022.
776 Taxonomical and functional composition of strawberry microbiome is genotype-dependent.
777 J. Adv. Res. 42, 189–204.
778 Scervino, J.M., Mesa, M.P., Della Mónica, I., Recchi, M., Sarmiento Moreno, N., Godeas, A.,
779 2010. Soil fungal isolates produce different organic acid patterns involved in phosphate salts
780 solubilization. Biol. Fertil. Soils 46, 755–763.

781 Segata, N., Izard, J., Waldron, L., Gevers, D., Miropolsky, L., Garrett, W.S., Huttenhower, C.,
782 2011. Metagenomic biomarker discovery and explanation. Genome Biol. 12, R60.
783 Song, X., Liu, M., Wu, D., Griffiths, B.S., Jiao, J., Li, H., Hu, F., 2015. Interaction matters: synergy
784 between vermicompost and PGPR agents improves soil quality, crop quality and crop yield
785 in the field. Appl. Soil Ecol. 89, 25–34.
786 Spohn, M., Kuzyakov, Y., 2013. Distribution of microbial- and root-derived phosphatase activities
787 in the rhizosphere depending on P availability and C allocation – coupling soil zymography
788 with ^{14}C imaging. Soil Biol. Biochem. 67, 106–113.
789 Tapia-Torres, Y., Rodríguez-Torres, M.D., Elser, J.J., Islas, A., Souza, V., García-Oliva, F.,
790 Olmedo-Álvarez, G., 2016. How to live with phosphorus scarcity in soil and sediment:
791 lessons from bacteria. Appl. Environ. Microbiol. 82, 4652–4662.
792 Tsai, H.-H., Schmidt, W., 2020. pH-dependent transcriptional profile changes in iron-deficient
793 *Arabidopsis* roots. BMC Genomics 21, 694.
794 Wang, S., Jiao, L.X., Yang, S., Jin, X., Yi, W., 2012. Effects of organic matter and submerged
795 macrophytes on variations of alkaline phosphatase activity and phosphorus fractions in lake
796 sediment. J. Environ. Manage. 113, 355–360.
797 Wu, S., Li, M., Zhang, C., Tan, Q., Yang, X., Sun, X., Pan, Z., Deng, X., Hu, C., 2021. Effects of
798 phosphorus on fruit soluble sugar and citric acid accumulations in citrus. Plant Physiol.
799 Biochem. 160, 73–81.
800 Xu Q, Ling N, Chen H, Duan Y, Wang S, Shen Q, Vandenkoornhuyse P., 2020. Long-term
801 chemical-only fertilization induces a diversity decline and deep selection on the soil bacteria.
802 Msystems. 5(4):10-128.

Xin, Y., Shi, Y., He, W.-M., 2022. A shift from inorganic to organic nitrogen-dominance shapes soil microbiome composition and co-occurrence networks. Front. Microbiol. 13, 1074064.

Yang, Q., Zhang, M., 2023. Effect of bio-organic fertilizers partially substituting chemical fertilizers on labile organic carbon and bacterial community of citrus orchard soils. Plant Soil 483, 255–272.

Yao, Q., Li, Z., Song, Y., Wright, S.J., Guo, X., Tringe, S.G., Tfaily, M.M., Paša-Tolić, L., Hazen, T.C., Turner, B.L., Mayes, M.A., Pan, C., 2018. Community proteogenomics reveals the systemic impact of phosphorus availability on microbial functions in tropical soil. Nat. Ecol. Evol. 2, 499–509.

Yin, X., Li, J., Shin, H., Du, G., Liu, L., Chen, J., 2015. Metabolic engineering in the biotechnological production of organic acids in the tricarboxylic acid cycle of microorganisms: Advances and prospects. Biotechnol. Adv. 33, 830–841.

Zhang, J., Li, Q., Qi, Y.P., Huang, W.L., Yang, L.T., Lai, N.W., Ye, X., Chen, L.S., 2018. Low pH-responsive proteins revealed by a 2-DE based MS approach and related physiological responses in Citrus leaves. BMC Plant Biol. 18, 188.

Zheng, M.M., Wang, C., Li, W.X., Song, W.F., Shen, R.F., 2019. Soil nutrients drive function and composition of phoC-harboring bacterial community in acidic soils of southern China. Front. Microbiol. 10.

Zhou, Y., Coventry, D.R., Gupta, V.V.S.R., Fuentes, D., Merchant, A., Kaiser, B.N., Li, J., Wei, Y., Liu, H., Wang, Y., Gan, S., Denton, M.D., 2020. The preceding root system drives the composition and function of the rhizosphere microbiome. Genome Biol. 21, 1–19.

Data Availability Statements

Raw data of 16S rRNA amplicon sequencing raw data used in this study are deposited in the NCBI database under BioProject PRJNA1067994, with accession number: SRR27710152-SRR27710175. Metagenomic sequensing raw data used in this study are dposited in the National Genomics Data Center (NGDC) database under BioProject PRJCA024813, with accession number: CRR1093803-CRR1093822. Other raw data is available on request.

Code Availability

The analysis code that supports the findings of this study is available on GitHub (https://github.com/wnq13579/organic_citrus_zxpsb)

Acknowledgements

Funding: This research was financially supported by the National Key Research and Development Program of China (grant number 2021YFD1600805), the China Agriculture Research System of MOF and MARA (grant number CARS-26), the National Natural Science Foundation of China (grant number 32102469), Special Fund for Youth Team of the Southwest University (grant number SWU-XJPY202308) and the Startup Fund of the Southwest University (grant number SWU-KQ22053).

Figures

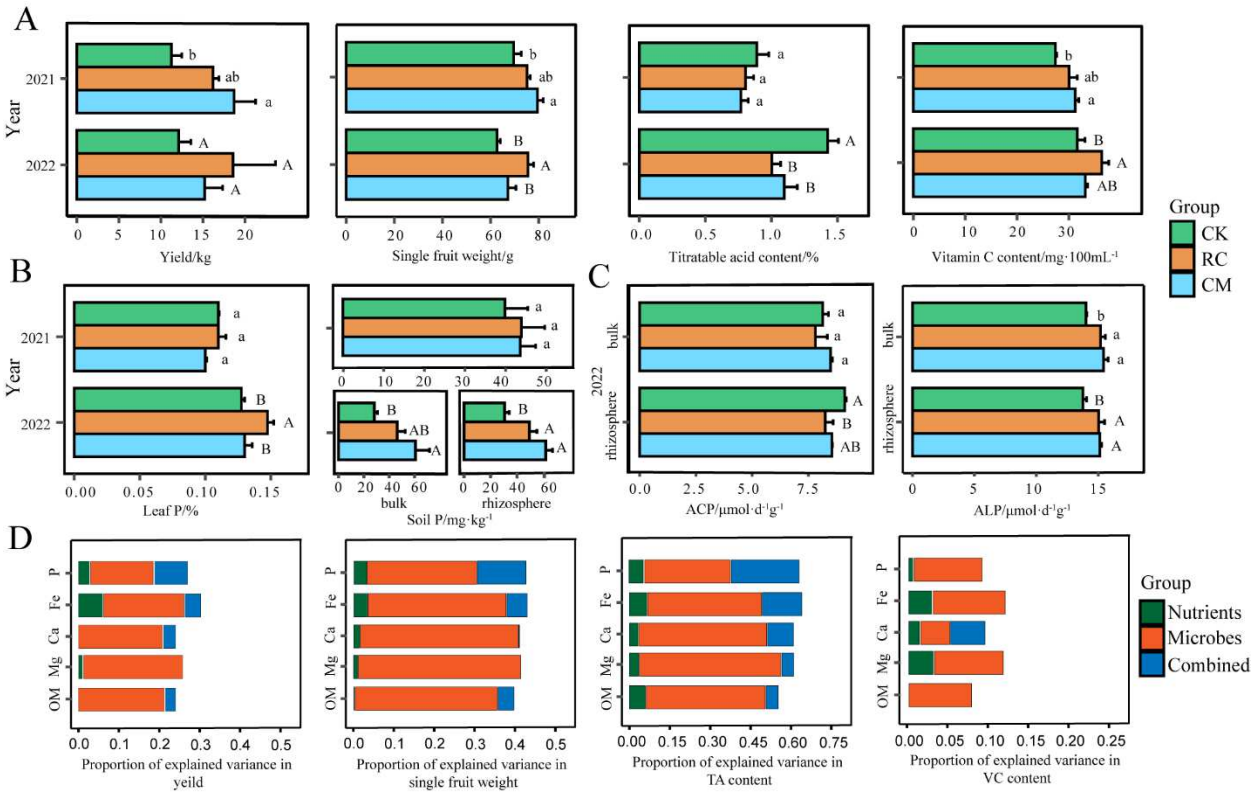


Fig. 1 Effect of organic fertilizer treatment on plant-soil performance of citrus. (A) Citrus yield and fruit quality after RC and CM treatments. (B) Plant and soil P nutritional levels after RC and CM treatments. (C) Soil enzyme activity of citrus after RC and CM treatments. (D) Individual and combined proportions of explained variance in yield, single-fruit weight, fruit titratable acidity (TA) and vitamin C, attributed to different nutrients (P, Fe, OM, etc.) and rhizosphere microbial community composition. Different lowercase letters indicate significant differences between treatments in 2021 (p<0.05), whereas different uppercase letters indicate significant differences between treatments in 2022 (p<0.05). Data are expressed as the mean ± SD, with n = 3 (2021, 3 biological replicates) and n = 4 (2022, 4 biological replicates).

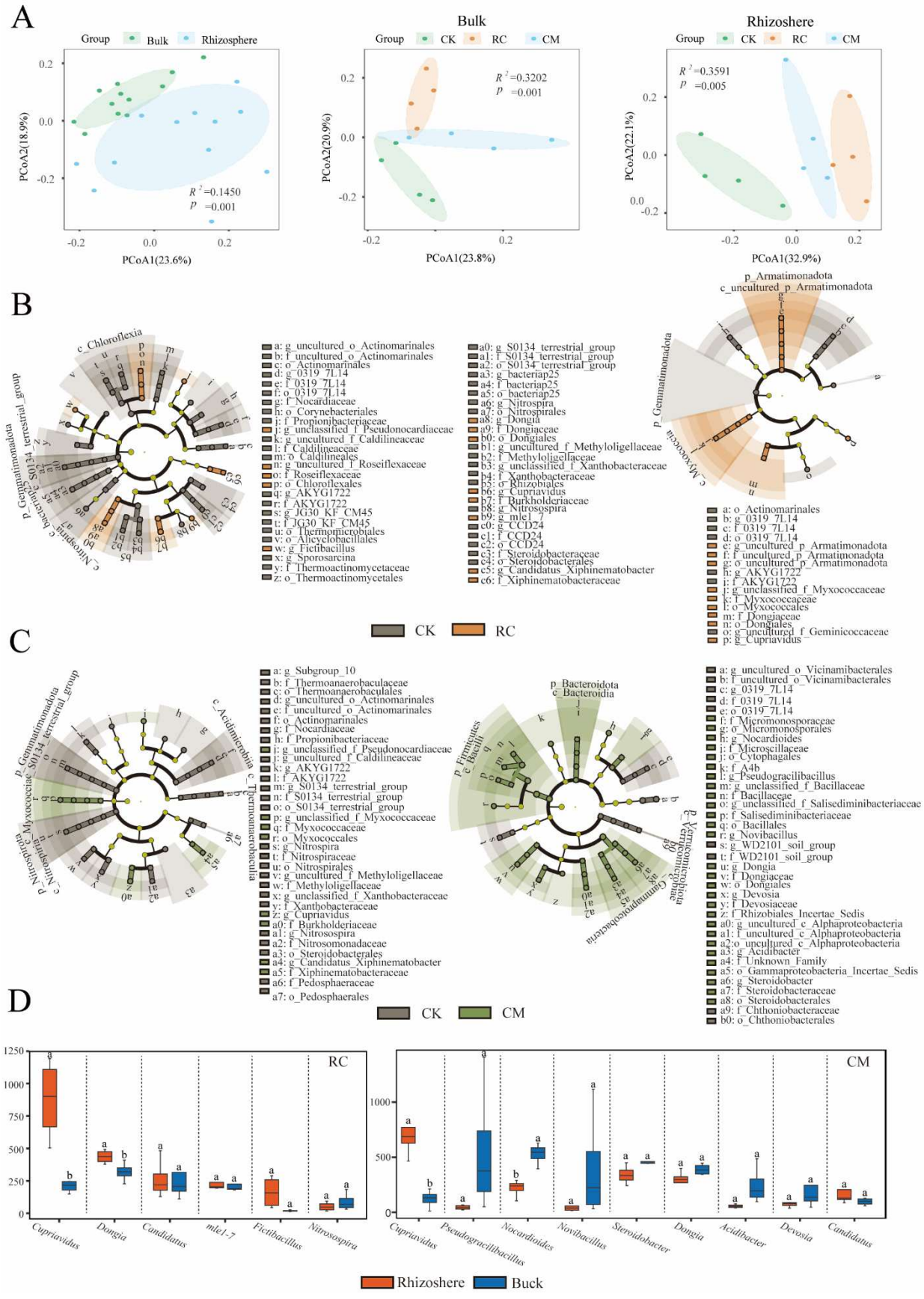

A
Group Bulk Rhizosphere
PCoA2(18.9%)
PCoA1(23.6%)
R^2=0.1450
p =0.001
Bulk
Group CK RC CM
PCoA2(20.9%)
PCoA1(23.8%)
R^2=0.3202
p =0.001
Rhizoshere
Group CK RC CM
PCoA2(22.1%)
PCoA1(32.9%)
R^2=0.3591
p =0.005
B
c_Chloroflexia
p_Gemmatimonadota
c_Gemmatimonadetes
c_Nitrospiria
p_Armatimonadota
c_uncultured_p_Armatimonadota
p_Gemmatimonadota
c_Myxococcia
a: g_uncultured_o_Actinomarinales
b: f_uncultured_o_Actinomarinales
c: o_Actinomarinales
d: g_0319_7L14
e: f_0319_7L14
f: o_0319_7L14
g: f_Nocardiaceae
h: o_Corynebacteriales
i: f_Propionibacteriaceae
j: g_unclassified_f_Pseudonocardiaceae
k: g_uncultured_f_Caldilineaceae
l: f_Caldilineaceae
m: o_Caldilineales
n: g_uncultured_f_Roseiflexaceae
o: f_Roseiflexaceae
p: o_Chloroflexales
q: g_AKYG1722
r: f_AKYG1722
s: g_JG30_KF_CM45
t: f_JG30_KF_CM45
u: o_Thermomicrobiales
v: o_Alicyclobacillales
w: g_Fictibacillus
x: g_Sporosarcina
y: f_Thermoactinomycetaceae
z: o_Thermoactinomycetales
a0: g_S0134_terrestrial_group
a1: f_S0134_terrestrial_group
a2: o_S0134_terrestrial_group
a3: g_bacteriap25
a4: f_bacteriap25
a5: o_bacteriap25
a6: g_Nitrospira
a7: o_Nitrospirales
a8: g_Dongia
a9: f_Dongiaceae
b0: o_Dongiales
b1: g_uncultured_f_Methyloligellaceae
b2: f_Methyloligellaceae
b3: g_unclassified_f_Xanthobacteraceae
b4: f_Xanthobacteraceae
b5: o_Rhizobiales
b6: g_Cupriavidus
b7: f_Burkholderiaceae
b8: g_Nitrosospira
b9: g_mle1_7
c0: g_CCD24
c1: f_CCD24
c2: o_CCD24
c3: f_Steroidobacteraceae
c4: o_Steroidobacterales
c5: g_Candidatus_Xiphinematobacter
c6: f_Xiphinematobacteraceae
a: o_Actinomarinales
b: g_0319_7L14
c: f_0319_7L14
d: o_0319_7L14
e: g_uncultured_p_Armatimonadota
f: f_uncultured_p_Armatimonadota
g: o_uncultured_p_Armatimonadota
h: g_AKYG1722
i: f_AKYG1722
j: g_unclassified_f_Myxococcaceae
k: f_Myxococcaceae
l: o_Myxococcales
m: f_Dongiaceae
n: o_Dongiales
o: g_uncultured_f_Geminicoccaceae
p: g_Cupriavidus
CK RC
C
p_Gemmatimonadota
c_Gemmatimonadetes
o_S0134_terrestrial_group
f_Myxococcaceae
c_Nitrospiria
p_Nitrospirota
c_Acidimicrobiia
c_Thermoanaerobaculia
p_Firmicutes
c_Bacilli
p_Bacteroidota
c_Bacteroidia
p_Verrucomicrobiota
c_Gammaproteobacteria
a: g_Subgroup_10
b: f_Thermoanaerobaculaceae
c: o_Thermoanaerobaculales
d: g_uncultured_o_Actinomarinales
e: f_uncultured_o_Actinomarinales
f: o_Actinomarinales
g: f_Nocardiaceae
h: f_Propionibacteriaceae
i: g_unclassified_f_Pseudonocardiaceae
j: g_uncultured_f_Caldilineaceae
k: g_AKYG1722
l: f_AKYG1722
m: g_S0134_terrestrial_group
n: f_S0134_terrestrial_group
o: o_S0134_terrestrial_group
p: g_unclassified_f_Myxococcaceae
q: f_Myxococcaceae
r: o_Myxococcales
s: g_Nitrospira
t: f_Nitrospiraceae
u: o_Nitrospirales
v: g_uncultured_f_Methyloligellaceae
w: f_Methyloligellaceae
x: g_unclassified_f_Xanthobacteraceae
y: f_Xanthobacteraceae
z: g_Cupriavidus
a0: f_Burkholderiaceae
a1: g_Nitrosospira
a2: f_Nitrosomonadaceae
a3: o_Steroidobacterales
a4: g_Candidatus_Xiphinematobacter
a5: f_Xiphinematobacteraceae
a6: f_Pedosphaeraceae
a7: o_Pedosphaerales
a: g_uncultured_o_Vicinamibacterales
b: f_uncultured_o_Vicinamibacterales
c: g_0319_7L14
d: f_0319_7L14
e: o_0319_7L14
f: f_Micromonosporaceae
g: o_Micromonosporales
h: g_Nocardioides
i: f_Microscillaceae
j: o_Cytophagales
k: f_A4b
l: g_Pseudogracilibacillus
m: g_unclassified_f_Bacillaceae
n: f_Bacillaceae
o: g_unclassified_f_Salisediminibacteriaceae
p: f_Salisediminibacteriaceae
q: o_Bacillales
r: g_Novibacillus
s: g_WD2101_soil_group
t: f_WD2101_soil_group
u: g_Dongia
v: f_Dongiaceae
w: o_Dongiales
x: g_Devosia
y: f_Devosiaceae
z: f_Rhizobiales_Incertae_Sedis
a0: g_uncultured_c_Alphaproteobacteria
a1: f_uncultured_c_Alphaproteobacteria
a2: o_uncultured_c_Alphaproteobacteria
a3: g_Acidibacter
a4: f_Unknown_Family
a5: o_Gammaproteobacteria_Incertae_Sedis
a6: g_Steroidobacter
a7: f_Steroidobacteraceae
a8: o_Steroidobacterales
a9: f_Chthoniobacteraceae
b0: o_Chthoniobacterales
CK CM
D
RC
CM
Cupriavidus
Dongia
Candidatus
mle1-7
Fictibacillus
Nitrosospira
Cupriavidus
Pseudogracilibacillus
Nocardioides
Novibacillus
Steroidobacter
Dongia
Acidibacter
Devosia
Candidatus
Rhizoshere Buck

Fig. 2 Organic fertilizer-induced alterations in microbial community diversity and composition. (A) Organic fertilizers altered microbial community diversity and composition. (B) LEfSe analysis of RC treatment and CK in rhizosphere soil (left) and bulk soil (right). (C) LEfSe analysis of CM treatment and CK control in rhizosphere soil (left) and bulk soil (right). Circles radiating from inside to outside represent the classification level from phylum to genus. Species without significant differences were uniformly colored yellow, and the significantly different species were colored according to the group. (D) The abundance of the enriched genera in the rhizosphere and non-rhizosphere soils. Data are expressed as the mean ± SD (n = 4, with n representing four biological replicates).

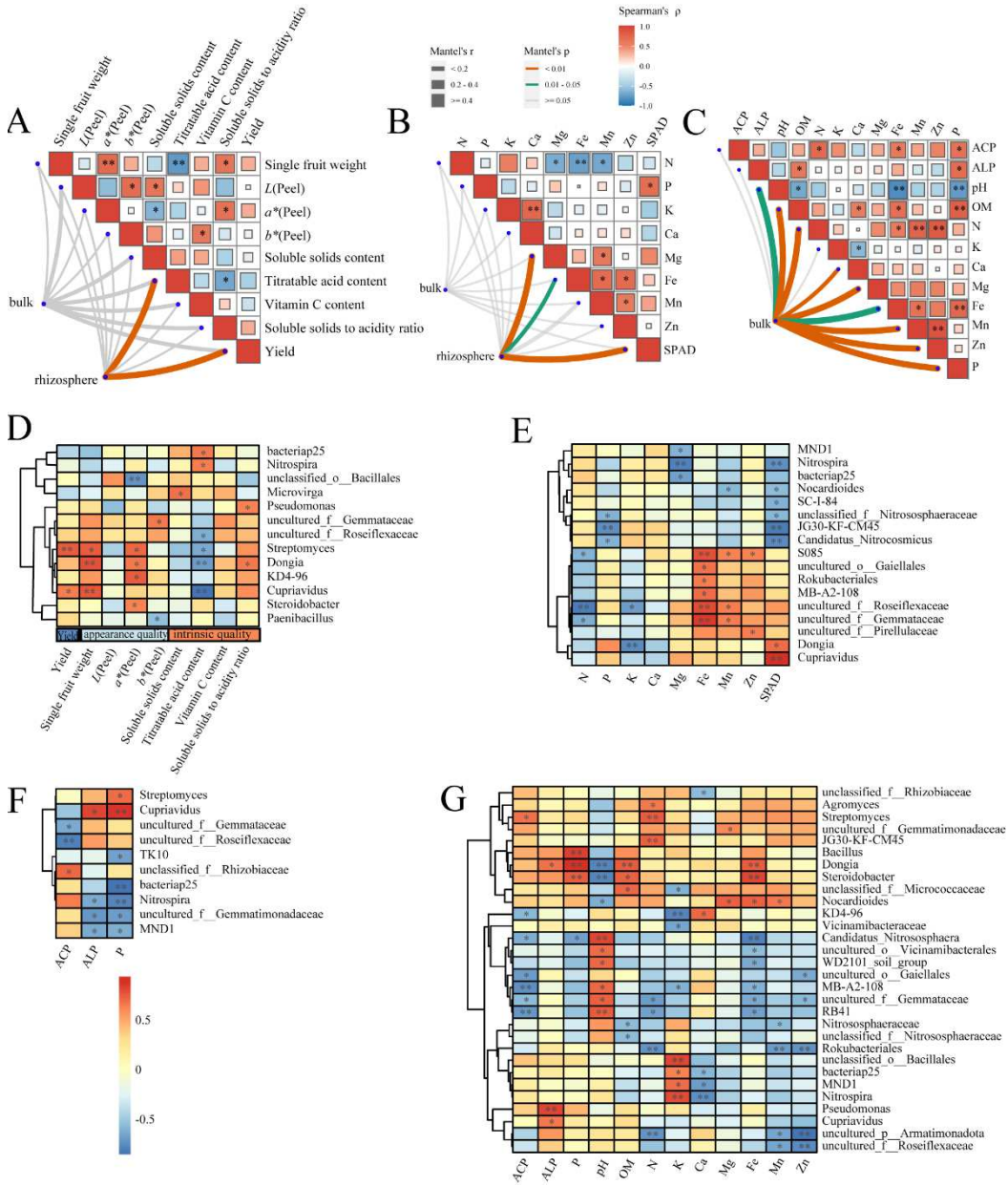
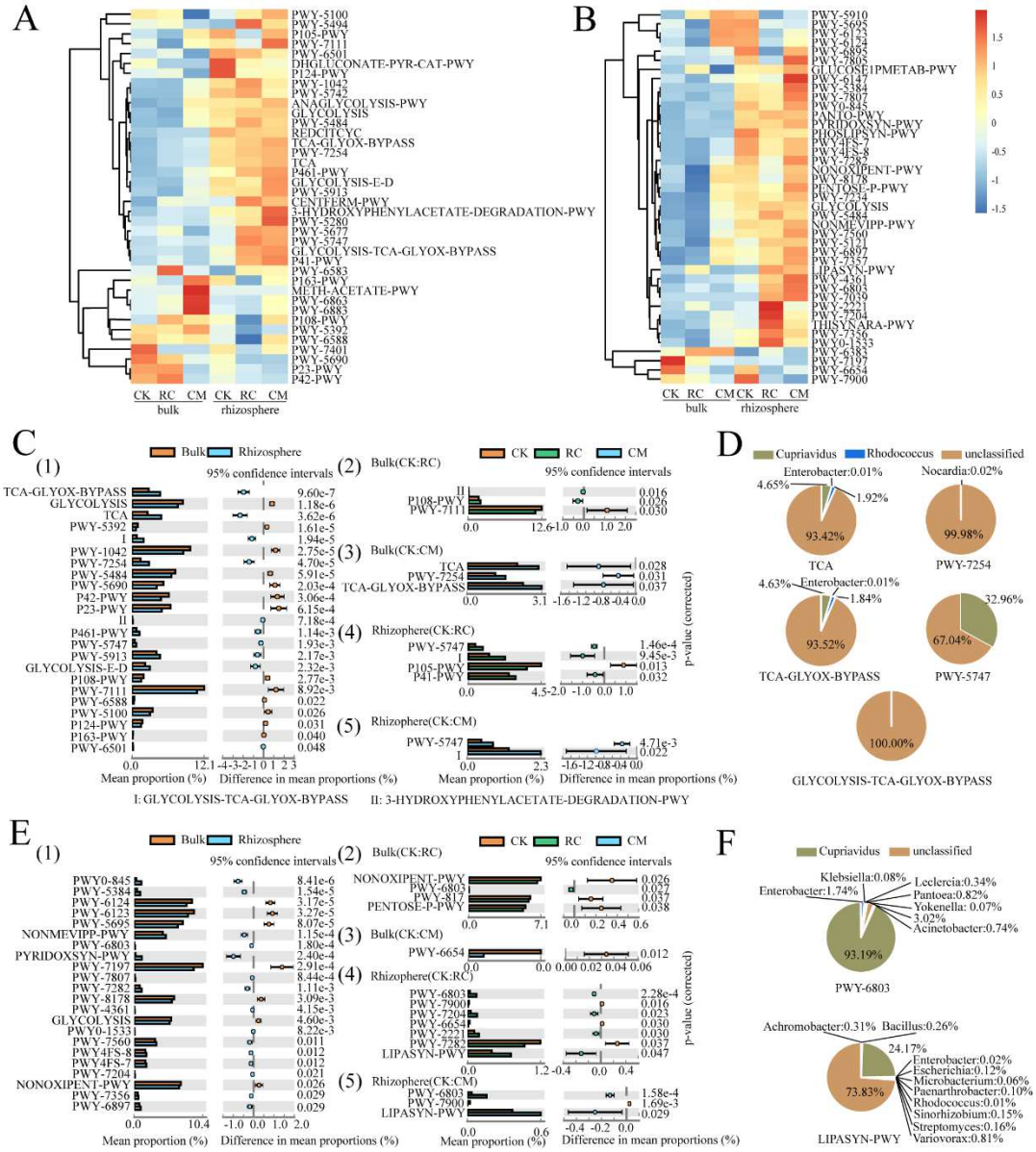


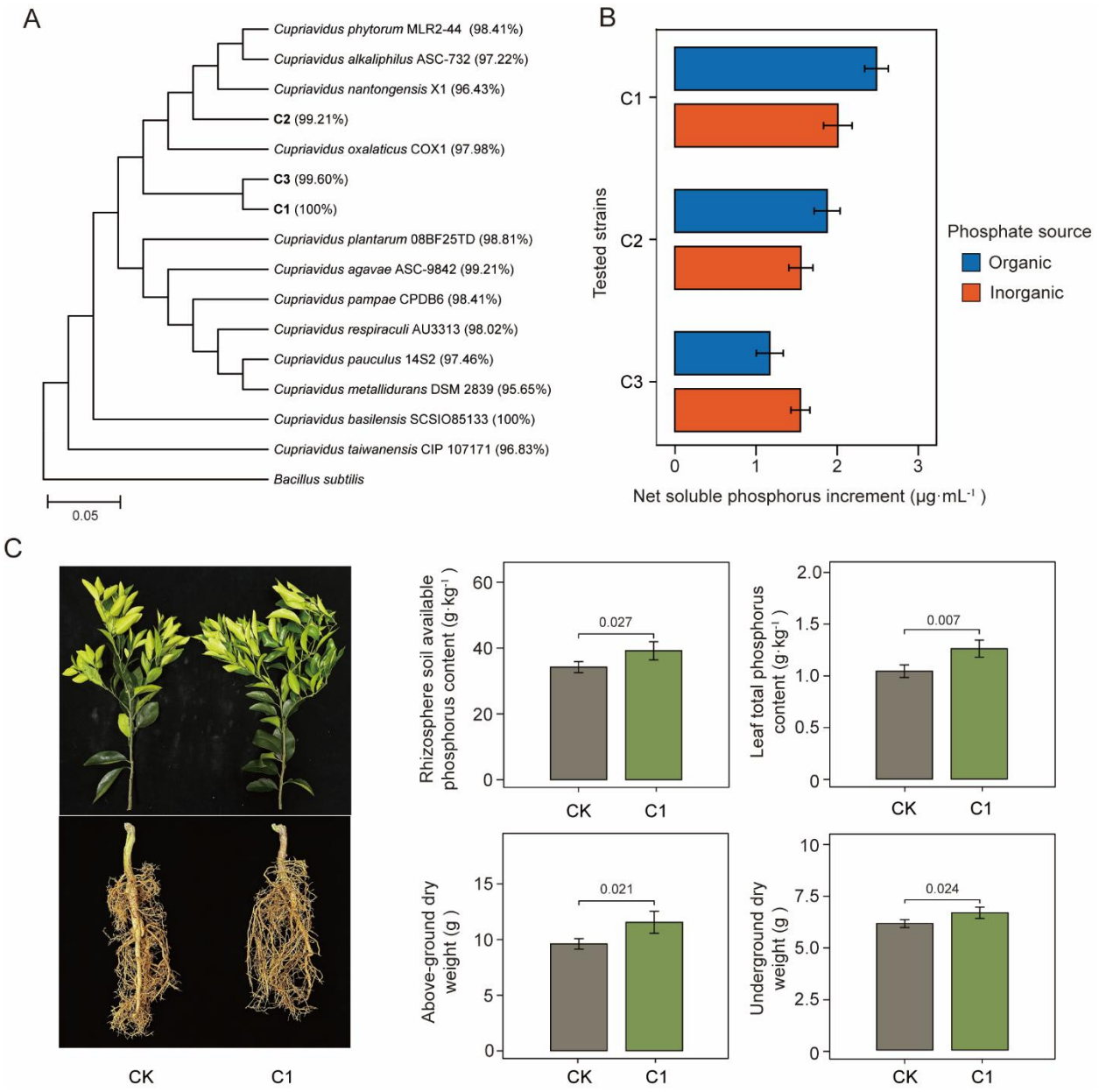
Fig. 3 Correlation coefficient matrix between plant and soil performance of citrus and microbial community. (A) Correlation coefficient matrix between fruit quality and microbial community. (B) Correlation coefficient matrix between leaf nutrition and microbial community. (C) Correlation coefficient matrix between soil physicochemical properties and microbial community. (D) Correlation between genus-level bacteria and fruit quality in rhizosphere soil. (E) Correlation between genus-level bacteria and leaf nutrition in rhizosphere soil. (F) Correlation

between genus-level bacteria and soil physicochemical properties in rhizosphere soil. (G) Correlation between genus-level bacteria and soil physicochemical properties in bulk soil.



872 **Fig. 4 Heatmap of metabolic pathways and pathway differential analysis under different**
873 **treatment.** (A) Heatmap of abundance after standardization of acid-related and (B) phosphorus-
874 related metabolic pathways under organic fertilizer treatments; (C) acid-related and (E)
875 phosphorus-related differential pathway analysis for different positions; (D) acid-related and (F)
876 phosphorus-related pathway composition analysis.

877



878

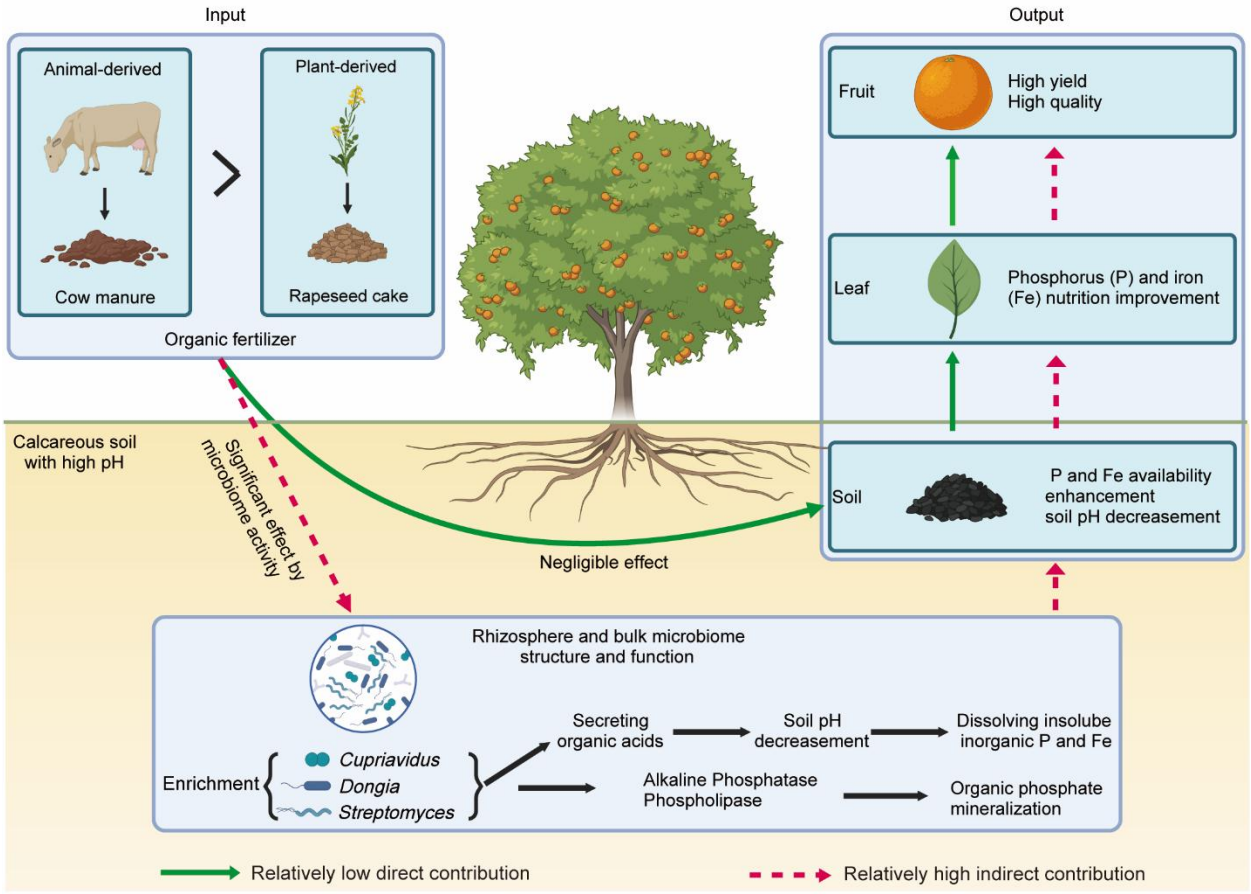
879 **Fig. 5 Screening and verification of candidate strains.** (A) Phylogenetic tree of three isolated

880 *Cupriavidus* strains and different species within the same genus. (B) Phosphate-solubilizing ability

881 of three *Cupriavidus* strains for organic and inorganic phosphorus. (C) Growth status of above-

882 ground and underground plant parts and related nutrient indicators in pot experiments. Data are

883 expressed as the mean ± SD (n = 4, with n representing four biological replicates).



884

885 **Fig. 6 Schematic diagram of microbiome-mediated enhancement of soil P and Fe availability**

886 **by organic fertilizers for improving citrus fruit quality**

Supplementary Files

This is a list of supplementary files associated with this preprint. Click to download.

- Supplementaryfile.docx